

# Continuous time crystal from a spontaneous many-body Floquet state

J. R. M. de Nova and F. Sols

*Departamento de Física de Materiales, Universidad Complutense de Madrid, E-28040 Madrid, Spain*

(Dated: July 5, 2021)

We propose the concept of a spontaneous many-body Floquet state. This is a state that, in the absence of external periodic driving, still self-oscillates like in the presence of a Floquet Hamiltonian, this behavior being spontaneously induced by many-body interactions. Furthermore, we prove that it is also a time crystal, presenting long-range time-periodic order. However, its time crystalline behavior is very different to that of conventional Floquet discrete time crystals: here, there is no external periodic driving, and the nature of the spontaneous symmetry breaking is continuous instead of discrete. We also demonstrate that a spontaneous many-body Floquet state can be implemented in a one-dimensional flowing atom condensate, resulting from a dynamical phase transition and stable against quantum fluctuations, and propose realistic experimental scenarios for its observation. The realization of a spontaneous many-body Floquet state would then not only provide a novel form of ordered quantum matter, but also a continuous time crystal.

*Introduction.*—Floquet driven systems [1–3], described by Hamiltonians with external periodic fields, provide very rich scenarios to study out-of-equilibrium features such as prethermalization [4], induced topological insulators [5], dynamical phase transitions [6] or high-harmonic generation [7]. An important application of Floquet driven systems arises in the context of time crystals. Originally proposed by Wilczek [8] as a system which exhibits a non-trivial time-periodic motion at equilibrium, it was later shown that the presented example of time crystal, based on a superconductor in a ring under the presence of a non-integer magnetic flux, was not the actual ground state [9]. Eventually, a no-go theorem ruling out time crystals as first conceived was proven in Ref. [10]. In that work, a more precise definition of a time crystal was provided: a system which at equilibrium exhibits long-range time-periodic order.

As a result of the no-go theorem, time crystals typically require out-of-equilibrium scenarios. An alternative route is provided by Floquet driven systems, where the spontaneous continuous symmetry breaking is reduced to a discrete one, manifested as a subharmonic response to the external periodic driving [11]. Floquet discrete time crystals have already been successfully achieved in setups as different as diamond nitrogen-vacancy centers [12], spin chains of ions [13], dipolar crystals [14], or atom condensates [15]. A related phenomenon is the time quasicrystal observed in magnon condensates, signaled by an incommensurate periodic response to the external Floquet driving [16–18].

Proposals for continuous time crystals have also been made. In that context, one way to evade the no-go theorem is a system with long-range interactions [19], or that is not in its actual ground state but rather in an excited eigenstate [20]. Dissipative time crystals in open quantum systems have been considered [21]. Boundary time crystals are also alternatives, where the crystalline behavior is observed at the system boundaries in the thermodynamic limit [22]. It was proposed that a genuine time

crystal could arise within an interacting gauge model in a Bose-Einstein condensate [23], but once more the setup was proven not to be in the actual ground state [24]. Moreover, classical time crystals are plausible [25, 26].

Here we propose the concept of a spontaneous many-body Floquet (SMBF) state, a state whose original Hamiltonian is time-independent, but in which many-body interactions spontaneously set the effective Hamiltonian determining the time-evolution to be periodic, and self-consistently the quantum state oscillates as a Floquet state. We also propose its realization in a one-dimensional atomic flowing condensate, and describe realistic experimental scenarios for its observation. Furthermore, we prove that an SMBF state presents time crystalline order, although in a manner completely different from conventional discrete Floquet time crystals, since there the system is externally driven with an imposed period and the symmetry breaking is discrete, not continuous.

*Spontaneous many-body Floquet state.*—First, we define the concept of an SMBF. For simplicity, we focus on the case of a Bose-Einstein condensate close to  $T = 0$ , which can be accurately described using a mean-field picture. Specifically, the dynamics of the condensate is described by the Gross-Pitaevskii (GP) equation  $i\hbar\partial_t\Psi(\mathbf{x}, t) = H_{\text{GP}}(\mathbf{x}, t)\Psi(\mathbf{x}, t)$ , with

$$H_{\text{GP}}(\mathbf{x}, t) = -\frac{\hbar^2}{2m}\nabla^2 + V(\mathbf{x}) + g|\Psi(\mathbf{x}, t)|^2, \quad (1)$$

$m$  being the mass of the atoms,  $V(\mathbf{x})$  some *time-independent* external potential and  $g$  the coupling constant. The operator  $H_{\text{GP}}(\mathbf{x}, t)$  is the nonlinear effective GP Hamiltonian which governs the dynamics, similar to the usual single-particle Schrödinger Hamiltonian operator but with an extra nonlinear term, arising from the interactions between the condensate atoms. Thus, if the external potential is stationary, the only possible time-dependence of  $H_{\text{GP}}(\mathbf{x}, t)$  comes from this interacting term. In addition, the system possesses an actual

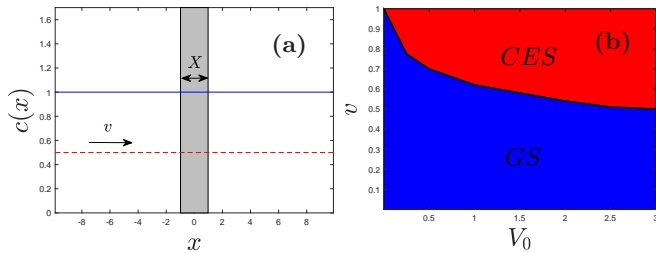


FIG. 1: (a) Spatial profile of sound (solid blue) and flow (dashed red) velocities of the IHFC, where the shaded area represents the region in which an attractive constant potential  $V(x) = -V_0$  is present. (b) Phase diagram for the final state of (a) for fixed  $X = 2$ .

Hamiltonian from where the equations of motion can be derived,

$$H = \int dx \frac{\hbar^2}{2m} |\nabla \Psi(\mathbf{x}, t)|^2 + V(\mathbf{x}) |\Psi(\mathbf{x}, t)|^2 + \frac{g}{2} |\Psi(\mathbf{x}, t)|^4 \quad (2)$$

and which is a conserved quantity as  $V(\mathbf{x})$  is stationary.

Now, we assume that the condensate density  $\rho(\mathbf{x}, t) = |\Psi(\mathbf{x}, t)|^2$  oscillates periodically with period  $T$ . In that case,  $H_{\text{GP}}(\mathbf{x}, t)$  takes the form of a Floquet Hamiltonian due to the nonlinear interacting term. Self-consistently, the wave function behaves like a Floquet state:

$$\Psi(\mathbf{x}, t) = u(\mathbf{x}, t) e^{-i\tilde{\mu}t/\hbar}, \quad u(\mathbf{x}, t) = \sum_{n=-\infty}^{\infty} u_n(\mathbf{x}) e^{-in\omega_0 t} \quad (3)$$

with  $u(\mathbf{x}, t + T) = u(\mathbf{x}, t)$ ,  $\omega_0 = 2\pi/T$  and  $\tilde{\mu}$  the *quasi-chemical potential*, which as usual is well-defined modulo the frequency  $\omega_0$ . The self-consistent nonlinear Floquet Hamiltonian then reads

$$H_{\text{GP}}(\mathbf{x}, t) = \left[ -\frac{\hbar^2}{2m} \nabla^2 + V(\mathbf{x}) + \rho(\mathbf{x}, t) \right] \quad (4)$$

$$\rho(\mathbf{x}, t) = \sum_{n=-\infty}^{\infty} \left[ \sum_{m=-\infty}^{\infty} u_m^*(\mathbf{x}) u_{n+m}(\mathbf{x}) \right] e^{-in\omega_0 t}$$

When inserted into the GP equation, this gives for each Floquet component  $u_n(x)$ ,

$$[\tilde{\mu} + n\omega_0] u_n(\mathbf{x}) = \left[ -\frac{\hbar^2}{2m} \nabla^2 + V(\mathbf{x}) \right] u_n(\mathbf{x}) \quad (5)$$

$$+ \sum_{m=-\infty}^{\infty} \sum_{k=-\infty}^{\infty} u_k^*(\mathbf{x}) u_{k+n-m}(\mathbf{x}) u_m(\mathbf{x})$$

which is a genuine nonlinear problem, resembling the Hartree-Fock equations [27].

We will refer to such a state as an SMBF state since a) the effective Hamiltonian  $H_{\text{GP}}(\mathbf{x}, t)$  is a Floquet Hamiltonian with a *well-defined* period  $T$ ,  $H_{\text{GP}}(\mathbf{x}, t + T) = H_{\text{GP}}(\mathbf{x}, t)$ , and the GP wave function has the form of a

Floquet state, and b) this periodic behavior is spontaneously induced by many-body interactions and not by some external driving. By well-defined period we understand that the period is unique and cannot be tuned by some symmetry transformation. In particular, we will exclude from our definition stationary *spatially* periodic solutions (like a cnoidal wave), since there a Galilean transformation of velocity  $w$  will induce a trivial time-periodic oscillation with  $T = a/w$ ,  $a$  being the lattice period, that can be arbitrarily tuned with  $w$ . This problem is avoided in the presence of an external stationary potential because it fixes a natural reference frame.

Since it breaks the continuous time translation symmetry, which is reduced to a discrete one, an SMBF state is also a time crystal. Specifically, in a condensate, the one-body correlation function already displays spatial off-diagonal long-range order and then

$$G(\mathbf{x}, \mathbf{x}', t, t') \equiv \langle \hat{\Psi}^\dagger(\mathbf{x}, t) \hat{\Psi}(\mathbf{x}', t') \rangle \simeq \Psi^*(\mathbf{x}, t) \Psi(\mathbf{x}', t') \quad (6)$$

exhibits a time-periodic behavior as a function of  $t$  when  $|\mathbf{x} - \mathbf{x}'| \rightarrow \infty$  [except for a trivial phase factor  $e^{i\tilde{\mu}(t-t')/\hbar}$ ], which is precisely the definition of long-range time periodic order.

*CES state.*—The question is now: does a non-trivial SMBF state exist? We identify here one example using a model previously studied in the literature [28], consisting of a 1D initially homogeneous flowing condensate (IHFC) with density  $n_0$  and velocity  $v$ , in which, at  $t = 0$ , an attractive square well of amplitude  $-V_0$  and size  $X$  is suddenly introduced. A schematic representation of the IHFC at  $t = 0$  is given in Fig. 1a. Hereafter we set units  $\hbar = m = c_0 = 1$  and rescale the GP wave function as  $\Psi(x, t) \rightarrow \sqrt{n_0} \Psi(x, t)$  so that it becomes dimensionless, with  $c_0 = \sqrt{gn_0/m}$  the initial speed of sound.

The quench in the external potential induces a deterministic dynamics in the condensate, numerically computed by integrating the time-dependent GP equation. Specifically, there are only two possible choices for the final state of the system as a function of the parameters  $(v, X, V_0)$ : the ground state (GS), or a periodic regime of continuous emission of solitons (CES) [28]. A typical phase diagram is represented in Fig. 1b.

We extend here the study of the CES state to prove that it is actually an SMBF state. Figures 2a,c show the condensate density  $|\Psi(x, t)|^2$  of the CES state. We observe that, after some transient features (blue circles), the system tends to accumulate particles in the well to reach GS (vertical white stripe placed within the well, centered at  $x = 0$ ). In order to conserve the particle number, a soliton is emitted upstream ( $x < 0$ ); however, in the CES state such a soliton is dragged back to the well (half dark rings on the left of the main white stripe), passing to the downstream ( $x > 0$ ) region and travelling with the flow (parallel diagonal black lines downstream). All this process is accompanied by the emission of waves

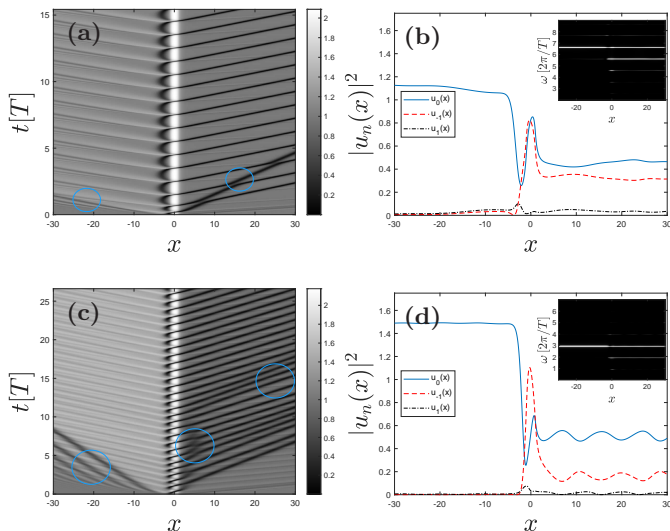


FIG. 2: Analysis of the CES state. Upper row: simulation with  $V_0 = 1$ ,  $X = 2$  and  $v = 0.65$ . (a) 2D plot of  $|\Psi(x,t)|^2$ . Time is in units of the CES period  $T$ . (b)  $|u_n(x)|^2$  for  $n = 0$  (solid blue),  $n = -1$  (dashed red) and  $n = 1$  (dashed-dotted black). Inset: Spectrum  $|\Psi(x,\omega)|^2$  once in the CES state, where  $\omega$  is in units of  $2\pi/T$ . (c)-(d) Same as first row but for a simulation with  $v = 0.95$ .

(parallel diagonal white lines upstream), which ensures the conservation of total particle number and energy.

The passage of the dragged soliton through the well leaves the system in the same configuration, and restarts the process described above. The resulting density pattern shows a periodic behavior for *every*  $x$ , and not just in the emitted trains of solitons (already noticed in the literature [28–30]). Therefore, since the whole density profile oscillates periodically, the effective GP Hamiltonian becomes a Floquet Hamiltonian. Self-consistently, the GP wave function behaves as a Floquet state, as can be seen from the Fourier transform of the wave function,  $\Psi(x,\omega)$ , displayed in the inset of Figs. 2b,d, which exhibits a discrete spectrum  $\Psi(x,\omega_n) = u_n(x)$ ,  $\omega_n = \bar{\mu} + n\omega_0$ . While the discrete lines are separated  $2\pi/T$ , there is some offset that reveals a non-trivial quasi-chemical potential. By taking the inverse Fourier transform around the spectrum peaks, we can recover each Floquet component  $u_n(x)$ , depicted in main Figs. 2b,d. The second row of Fig. 2 analyzes a simulation with larger flow velocity, which has a smaller period  $T$  and fewer dominant Floquet components.

We can proceed further and use the Floquet components to reconstruct the wave function by truncating the expansion of Eq. (3),

$$\Psi_N(x,t) = e^{-i\bar{\mu}t} \sum_{n=-N}^N u_n(x) e^{-in\omega_0 t} \quad (7)$$

where we are fixing the definition of the quasi-chemical potential so that the dominant component is  $u_{n=0}(x)$ .

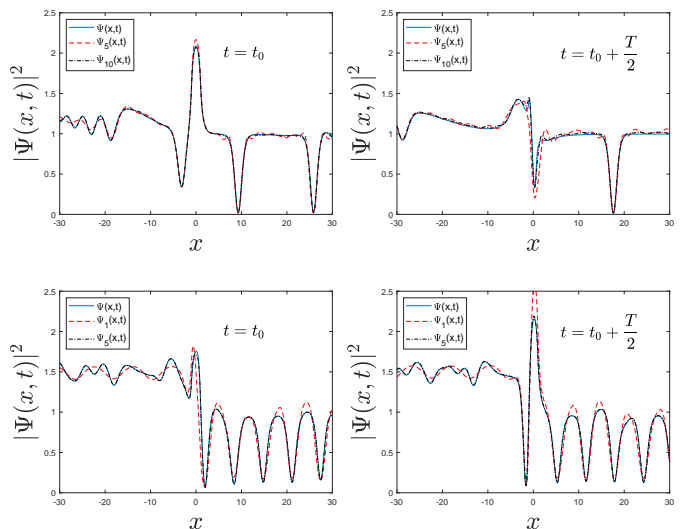


FIG. 3: Snapshots of the density  $|\Psi(x,t)|^2$  of the CES state (solid blue) and the truncated Floquet expansions  $\Psi_N(x,t)$  (dashed red and dashed-dotted black) from Eq. (7) during a period for the simulations of upper and lower row of Fig. 2, respectively, where the origin of times  $t_0$  is chosen arbitrarily.

Figure 3 compares the oscillation within a period of the actual CES wave function  $\Psi(x,t)$  with the reconstructed Floquet wave function  $\Psi_N(x,t)$ , where the latter is seen to rapidly converge for small values of  $N$ . We also see that, for lower flow velocities, more Floquet components are needed to reconstruct the CES state, as already expected from Fig. 2. This reconstruction explicitly demonstrates that the CES state is in fact an SMBF state.

*Time-crystal behavior.*—We characterize in detail the time crystalline properties of the CES state in Fig. 4. First, we compute the mean-field value of the correlation function  $G(x,x',t,t')$ , where we take the absolute value in order to suppress high-frequency features due to the background flow,  $\sim e^{-iv(x-x')}$ , and to the quasi-chemical potential,  $\sim e^{i\bar{\mu}(t-t')}$ . Figure 4a characterizes its spatial structure for  $t = t'$  and Fig. 4b its time structure for fixed spatial points far away, one upstream and one downstream. The correlation function clearly exhibits a time periodic behavior in both  $t, t'$  for distant points, revealing the time crystalline behavior.

Since the induced dynamics in the IHFC is deterministic, the time crystal is robust against the presence of quantum and thermal fluctuations, provided that they are sufficiently small. Technically speaking, off-diagonal long-range order of the one-body correlation function is destroyed in a 1D condensate by phase fluctuations, and one must speak of a 1D quasi-condensate. Specifically, at  $T = 0$  there is an algebraic decay with the distance, while for  $T > 0$  it becomes exponential [32]. Long-range order in time presents the same behavior [33]. However, the space-time decay can be neglected in typical experimen-

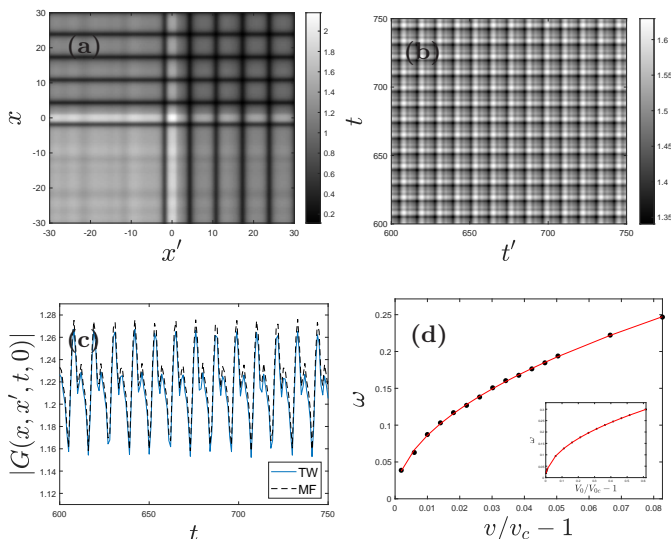


FIG. 4: Absolute value of the correlation function  $|G(x, x', t, t')|$  for the setup of lower Fig. 2. (a) Mean-field value for  $t = 610$  as a function of  $(x, x')$ . (b) Mean-field value for  $x = -30$  and  $x' = 30$  as a function of  $(t, t')$ . (c) Comparison of  $G(x, x', t, 0)$  for  $-x = x' = 50$  as a function of  $t$  between a Truncated Wigner simulation [31] that includes quantum fluctuations (solid blue) and the mean-field prediction (dashed-black). (d) Critical behavior of the CES frequency close to the phase transition with respect to the velocity  $v$  for  $V_0 = 1$ ,  $X = 2$ . The red line represents a fit to a power law. Inset: Same but with respect to the amplitude  $V_0$  for  $v = 0.62$ ,  $X = 2$ .

tal setups if the density and temperature are high and low enough, respectively, and a GP mean-field approximation describes accurately the condensate dynamics. Indeed, this approximation becomes exact in the limit  $g, T \rightarrow 0$ ,  $n_0 \rightarrow \infty$ , with  $gn_0$  constant, and is considered in other works on time crystals [8, 20, 23, 24]. In order to explicitly check the robustness against quantum fluctuations, we have carried out a simulation using the Truncated Wigner approximation [34, 35], finding that the long-range time periodic behavior of  $G(x, x', t, 0)$  survives for long times, as shown in Fig. 4c.

The GS/CES phase transition is an example of a dynamical phase transition, typical of setups in which a strong quench in an external parameter is introduced [36–38]. The GS is the symmetry unbroken phase, with continuous time translation symmetry, and the CES is the time crystal phase, with discrete time translation symmetry, where the order parameter describing the phase transition is the time Fourier transform of the correlation function  $G(x, x', t, 0)$ . A more quantitative description of the phase transition can be seen in Fig. 4d, where the CES frequency is shown to display a critical behavior close to the phase transition at the critical values  $v_c, V_{0c}$ , with the critical exponents associated to  $v, V_0$  being  $\alpha \simeq \beta \simeq 0.50$ , respectively. Qualitatively, the vanishing of the CES frequency arises because the GS/CES

phase transition occurs when the velocity of the upstream emitted soliton equals that of the background flow, so it takes the soliton an infinite amount of time to return to the well.

Nevertheless, a quench in the external potential is not the only way to reach the CES state: for fixed background parameters  $(v, X, V_0)$ , the CES state, and particularly its period, is insensitive to the details of the transient, including stochastic dynamics starting from unstable black-hole laser solutions [28, 30, 39]. This independence with respect to the transient further demonstrates that the CES state is indeed an intrinsic state of the system, satisfying Eq. (5). In particular, the time crystal can be reached without a previous periodic driving [16, 17].

In a discrete time crystal, rigidity is a signature of time crystalline behavior, since it demonstrates that the state is not due to some particular fine-tuning [12, 13]. In our case, the analogue phenomenon is the robustness of the time crystalline behavior against variations of the parameters  $(v, X, V_0)$ . As shown by the phase diagram in Fig. 1b, the SMBF state survives in a wide region of parameter space. The period varies continuously with  $(v, X, V_0)$ , but this is quite a natural feature arising from the continuous character of the spontaneous symmetry breaking considered here. On the other hand, many-body interactions are critical in the formation of the time crystal from the very beginning, since the periodicity is induced by the nonlinear term in Eq. (1), genuinely many-body.

The proposed time crystal is also universal (in the sense that it appears for a wide range of obstacles in a flowing condensate) and not restricted to an *idealized* square well. We have explicitly checked this by considering different potentials with realistic shapes or delta barriers, both attractive and repulsive. In all cases, we have found that a CES state is always achieved provided the flow velocity is high enough. While soliton trains in condensates appear in a variety of scenarios [29, 40–42], this is the first time that an SMBF state has been identified and characterized in this type of system.

The CES state persists indefinitely in the thermodynamic limit since we only observe its collapse in the numerical simulations due to the effect of the finite size of the system, when reflections at the boundaries come back and distort the dynamics. Based on this argument, the lifetime  $\tau$  of the CES state is expected to grow linearly with the size of the system  $L$ ,  $\tau \sim L$ . Therefore, in the thermodynamic limit, we expect our time crystal to survive indefinitely. Actually, in contrast to Floquet driven states, an SMBF state has a conserved energy, computed from Eq. (2). Specifically, for the CES state,  $E_{\text{CES}} = E_{\text{GS}} + O(1)$  and thus, in the thermodynamic limit,  $\lim_{N \rightarrow \infty} E_{\text{CES}}/N = \lim_{N \rightarrow \infty} E_{\text{GS}}/N$ . However, separately in both the upstream and downstream regions the change in number of particles and energy with respect to the initial state is  $O(N)$ .

*Experimental implementation.*—Finally, we propose a simple and feasible experimental scheme for the characterization of the CES time crystal. We consider an elongated quasi-1D condensate that is essentially homogeneous far from the edges of the trap, in which a localized obstacle is swept with velocity  $v$  along the condensate. By Galilean invariance, this is equivalent to launching the condensate against the obstacle. If the velocity is high enough, after some transient the system will reach the CES state. Indeed, soliton trains have already been observed in similar setups [41], which hints at an underlying SMBF state. We suggest to extend this type of experiment to follow in detail the periodic time evolution of the system, including both the upstream and downstream regions, by employing high-resolution imaging to measure the density profile in the obstacle frame, in a similar way to recent experiments in analog gravity [43–45]. Another possibility could be to confine a condensate in a long ring [46] and rotate a localized potential.

*Conclusions and outlook.*—We have proposed a novel form of quantum state: an SMBF state. Using a flowing atomic condensate, we have identified a particular realization of such a state, described by a dynamical phase diagram and robust against quantum fluctuations, and designed a realistic experimental scenario for its implementation. An SMBF state extends the physics of nonlinear Floquet waves [17, 18] to scenarios without external periodic driving. Apart from the intrinsic conceptual interest and potential applications, an SMBF state is a particular example of a continuous time crystal.

The idea of SMBF state could also be extended to other systems obeying similar nonlinear equations of motion, such as nonlinear optical fibers [47], quantum fluids of light [48], or superconductors [49], and to fermionic systems described by mean-field approaches, as for instance the Hartree-Fock equations [27], the fermionic analog of the GP equation.

We are grateful to I. Carusotto for stimulating discussions. We also thank C. Creffield, I. Zapata, S. Finazzi, F. Michel and R. Parentani, to whose memory we devote this work, for useful comments, especially during the visit of one of us (JRMdN) to Université Paris-Saclay. This work has been supported by Grant FIS2017-84368-P from Spain’s MINECO.

---

[1] J. H. Shirley, Phys. Rev. **138**, B979 (1965).

[2] H. Sambi, Phys. Rev. A **7**, 2203 (1973).

[3] M. Grifoni and P. Hänggi, Physics Reports **304**, 229 (1998).

[4] P. Peng, C. Yin, X. Huang, C. Ramanathan, and P. Cappellaro, Nature Physics **17**, 444 (2021).

[5] N. H. Lindner, G. Refael, and V. Galitski, Nature Physics **7**, 490 (2011).

[6] T. c. v. Prosen and E. Ilievski,

Phys. Rev. Lett. **107**, 060403 (2011).

[7] Y. Murakami, M. Eckstein, and P. Werner, Phys. Rev. Lett. **121**, 057405 (2018).

[8] F. Wilczek, Phys. Rev. Lett. **109**, 160401 (2012).

[9] P. Bruno, Phys. Rev. Lett. **110**, 118901 (2013).

[10] H. Watanabe and M. Oshikawa, Phys. Rev. Lett. **114**, 251603 (2015).

[11] D. V. Else, B. Bauer, and C. Nayak, Phys. Rev. Lett. **117**, 090402 (2016).

[12] S. Choi, J. Choi, R. Landig, G. Kucsko, H. Zhou, J. Isoya, F. Jelezko, S. Onoda, H. Sumiya, V. Khemani, *et al.*, Nature **543**, 221 (2017).

[13] J. Zhang, P. Hess, A. Kyprianidis, P. Becker, A. Lee, J. Smith, G. Pagano, I.-D. Potirniche, A. C. Potter, A. Vishwanath, *et al.*, Nature **543**, 217 (2017).

[14] J. Rovny, R. L. Blum, and S. E. Barrett, Phys. Rev. Lett. **120**, 180603 (2018).

[15] J. Smits, L. Liao, H. T. C. Stoof, and P. van der Straten, Phys. Rev. Lett. **121**, 185301 (2018).

[16] S. Autti, V. B. Eltsov, and G. E. Volovik, Phys. Rev. Lett. **120**, 215301 (2018).

[17] A. J. E. Kreil, H. Y. Musiienko-Shmarova, S. Eggert, A. A. Serga, B. Hillebrands, D. A. Bozhko, A. Pomyalov, and V. S. L’vov, Phys. Rev. B **100**, 020406 (2019).

[18] N. Träger, P. Gruszecki, F. Lisiecki, F. Groß, J. Förster, M. Weigand, H. Głowiński, P. Kuświk, J. Dubowik, G. Schütz, M. Krawczyk, and J. Gräfe, Phys. Rev. Lett. **126**, 057201 (2021).

[19] V. K. Kozin and O. Kyriienko, Phys. Rev. Lett. **123**, 210602 (2019).

[20] A. Syrwid, J. Zakrzewski, and K. Sacha, Phys. Rev. Lett. **119**, 250602 (2017).

[21] C. Booker, B. Buča, and D. Jaksch, New Journal of Physics **22**, 085007 (2020).

[22] F. Iemini, A. Russomanno, J. Keeling, M. Schirò, M. Dalmonte, and R. Fazio, Phys. Rev. Lett. **121**, 035301 (2018).

[23] P. Öhberg and E. M. Wright, Phys. Rev. Lett. **123**, 250402 (2019).

[24] A. Syrwid, A. Kosior, and K. Sacha, Phys. Rev. Research **2**, 032038 (2020).

[25] A. Shapere and F. Wilczek, Phys. Rev. Lett. **109**, 160402 (2012).

[26] R. Hurtado-Gutiérrez, F. Carollo, C. Pérez-Espigares, and P. I. Hurtado, Phys. Rev. Lett. **125**, 160601 (2020).

[27] G. Giuliani, G. Vignale, A. Eringen, and C. U. Press, *Quantum Theory of the Electron Liquid*, Masters Series in Physics and Astronomy (Cambridge University Press, 2005).

[28] J. R. M. de Nova, P. F. Palacios, I. Carusotto, and F. Sols, New Journal of Physics **23**, 023040 (2021).

[29] V. Hakim, Phys. Rev. E **55**, 2835 (1997).

[30] J. R. M. de Nova, S. Finazzi, and I. Carusotto, Phys. Rev. A **94**, 043616 (2016).

[31] The parameters of the Truncated Wigner simulation are those of lower Fig. 2, using a condensate in a ring at  $T = 0$  with  $N = 10^8$  and  $L \simeq 1885$ ; see Ref. [28] for the details. The number of modes is  $N_m = 3000$ , which corresponds to a cut-off  $|k| \leq 5$ .

[32] L. Pitaevskii and S. Stringari, *Bose-Einstein Condensation and superfluidity* (Clarendon Press, Oxford, 2016).

[33] This is easily seen for a homogeneous condensate by noting that phase fluctuations diverge in the infrared as

- $\sim \int dk k^{-r} (1 - \cos [k(x - x') - c_0|k|(t - t')]) / 4\pi n_0 \xi_0$ ,  
with  $r = 1$  for  $T = 0$  and  $r = 2$  for  $T > 0$ .
- [34] A. Sinatra, C. Lobo, and Y. Castin, *J. Phys. B: At. Mol. Opt. Phys* **35**, 3599 (2002).
- [35] I. Carusotto, S. Fagnocchi, A. Recati, R. Balbinot, and A. Fabbri, *New J. Phys.* **10**, 103001 (2008).
- [36] M. Moeckel and S. Kehrein, *Phys. Rev. Lett.* **100**, 175702 (2008).
- [37] B. Sciolla and G. Biroli, *Phys. Rev. Lett.* **105**, 220401 (2010).
- [38] J. Lang, B. Frank, and J. C. Halimeh, *Phys. Rev. Lett.* **121**, 130603 (2018).
- [39] F. Michel and R. Parentani, *Phys. Rev. A* **91**, 053603 (2015).
- [40] N. Pavloff, *Phys. Rev. A* **66**, 013610 (2002).
- [41] P. Engels and C. Atherton, *Phys. Rev. Lett.* **99**, 160405 (2007).
- [42] J. H. V. Nguyen, D. Luo, and R. G. Hulet, *Science* **356**, 422 (2017).
- [43] J. Steinhauer, *Nature Phys.* **12**, 959 (2016).
- [44] J. R. M. de Nova, K. Golubkov, V. I. Kolobov, and J. Steinhauer, *Nature* **569**, 688 (2019).
- [45] V. I. Kolobov, K. Golubkov, J. R. M. de Nova, and J. Steinhauer, *Nature Physics* (2021).
- [46] S. Eckel, A. Kumar, T. Jacobson, I. B. Spielman, and G. K. Campbell, *Phys. Rev. X* **8**, 021021 (2018).
- [47] P. D. Drummond and M. Hillery, *The quantum theory of nonlinear optics* (Cambridge University Press, 2014).
- [48] I. Carusotto and C. Ciuti, *Reviews of Modern Physics* **85**, 299 (2013).
- [49] J. S. Langer and V. Ambegaokar, *Phys. Rev.* **164**, 498 (1967).